

# Minimization of the shape error in the interrupted grinding process by using Taguchi method

M. Kurt\*, U. Köklü\*\*

\*University of Marmara, 34722 İstanbul, Turkey

\*\*University of Dumlupınar, 43500 Simav, Kütahya, Turkey, E-mail: ugurkoklu@gmail.com

crossref <http://dx.doi.org/10.5755/j01.mech.18.6.3163>

## 1. Introduction

Higher productivity and better surface quality are the prerequisites for current machining industry to be more competitive since modern manufacturing processes require shorter production time and higher precision components [1]. Grinding, wherein the abrasives are bonded together into the wheel, is the most common abrasive machining process. In this process, metal is removed from the workpiece by the mechanical action of irregularly shaped abrasive grains [2]. Since grinding is a high-energy rate metal cutting process, thermal analysis is important for the concerns of the workpiece, such as phase transformation, residual stresses, thermal cracks, burn marks, variations in hardness and geometrical error. Among all of these, shape error is the most concern in precision grinding, since it largely decreases the yield rate of the workpiece. The main factors affecting geometrical accuracy include the local thermal deformation of the workpiece, wheel (grain) deformation, workpiece deformation subject to the grinding force, deflection of the wheel spindle and clearance between the spindle and the bearing. Many researchers have been studied the geometrical error and pointed out that the thermal deformation causes a serious concavity on the ground profile [3-8].

The effect of grinding parameters on the geometric error was evaluated and optimum grinding conditions for minimizing the geometric error were determined by Kwak [9], Kwak and Kim [10]. The results of their experiment indicate that, the grinding depth was a dominant parameter for geometric error and the next was the wheel grain size. Ohmoriet al. [11] investigated the deformation behaviors of the sintered SiC workpiece during the grinding process. They have indicated that, the maximum value of the profile deformation is about 0.33  $\mu\text{m}$ . Sosa et al. [12] studied surface roughness, residual stress and shape distortion of ductile iron plates. They concluded that, sample distortion consisted in a longitudinally oriented curvature, of concave shape on the ground side.

The literature regarding geometric error has been summarized above. However, a very few published works are available on the effect of grinding parameters on shape error in interrupted grinding. In this study the mentioned point has been taken into account and aimed to reduce the shape error of GS-C25 cast steel materials, used in valves which serve for transmitting and storing of high temperature and pressurized liquids. The main goal of this experimental investigation is to determine the effects of wheel and cutting parameters on shape error in interrupted grinding. Taguchi method was used to accomplish the objective. Mathematical models fitted to the experimental data will

contribute towards the selection of the optimum process conditions.

## 2. Shape error in interrupted surface grinding

The grinding process is generally used as a final stage of the metallic materials machining to have necessary surface quality and measurement. Since grinding process costs much, it should be done carefully. If workpiece's surface shape in surface grinding is examined, it will be noticed that instead of a smooth surface there will be cavity dependent on grinding wheel's radius. Grinding wheel's geometrical size, its wear and grinding force will have an effect on these shape errors. In addition to above mentioned causes, pockets, holes and slots constituted interrupted surface on the workpieces, increase the shape error. As a result, surface shape errors form around the discontinuities. During grinding process, the most important cause of shape error in interrupted surfaces is elastic displacement change which is an effect of cutting force. The effect of these forces of severity depends on the effect of abrasive particles to the surface (workpiece), the geometrical size of grinding wheel, the relative displacement speed of workpiece and the size of contact area of abrasive. Investigation of the shape errors of grinding surfaces are very crucial in manufacturing in order to reduce or to get rid of these errors. In the components with shape errors, one can face with undesirable cases such as fault of sealing, reduction in components' contact surfaces, wear and reduction of proper working life of components. In addition to this, after assembling the ground components, the shape errors around holes may cause the cavity that can lead to leaking of high pressurized liquids or gas. In Fig. 1 an example of the measured geometric error was shown [10].

## 3. Experimental setup and design

Chemical composition and mechanical properties of GS-C25 cast steel are presented in Table 1. The experimental cast workpiece dimensions having stress relieving treatment are 205  $\times$  140  $\times$  30 mm.

Table 1  
Mechanical and chemical properties of GS-C25 cast steel

Tensile properties				
$\sigma_u$ , MPa	$\sigma_y$ , MPa	Elongation, %	Hardness, HB	
420 - 600	240	22	130 - 170	
Chemical compositions (wt%)				
C	Si	Mn	P	S
0.2	< 0.60	0.80	< 0.020	< 0.015

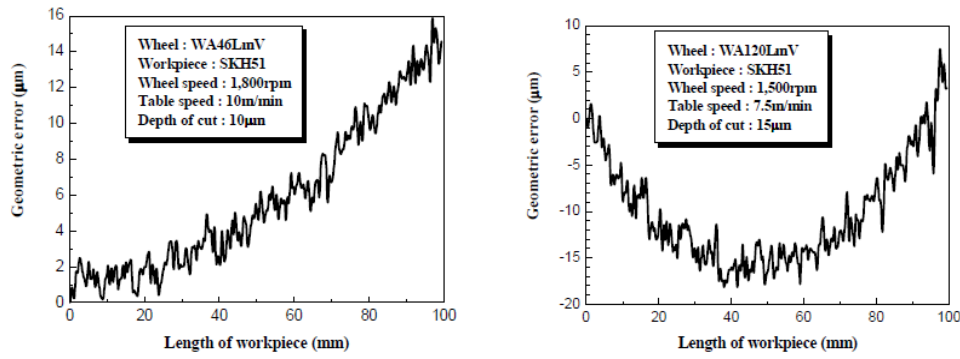


Fig. 1 Example of geometric error generated during grinding process

The workpiece material specimens having the size of  $203 \times 135 \times 28$  mm were prepared by milling and grinding. Square, circular and triangle pockets were cut into the specimen to provide the interrupted cutting conditions during grinding. But only the effect of circle on the shape error was investigated. The cast sample, machined surface, geometric shapes and size of the workpiece is shown in Fig. 2. Square (50 mm), circle (diameter of 50 mm) and triangle (isosceles triangle with altitude 50 mm) shapes from each sample were removed by a CNC wire electrical discharge machine (WEDM). WEDM process generally generates a significant amount of heat during the process. Prior to grinding experiment, to eliminate the heat affected zone the sample surface was roughly machined by grinding approximately to 1 mm. In the grinding experiments, a

universal grinding machine with aluminum oxide grinding wheels with dimensions of  $350 \times 40 \times 127$  mm and a constant wheel speed of 27 m/s is used. Furthermore, these elements are common. For example A-K-6-V means alumina grit, hardness K, structure 6 and vitrified bond. The selection was based on the wide industrial application of the grinding wheels. Four grinding wheels used in the experiments have different wheel grain size namely 36, 46, 60 and 80 mesh. Before each grinding experiment, the grinding wheel was dressed using a single-point diamond dresser to produce a sharp, clean wheel surface. During the grinding process, a water-soluble metalworking fluid diluted to 1:5 was supplied to the grinding zone, and the coolant flow rate from the outlet was 6 l/min.

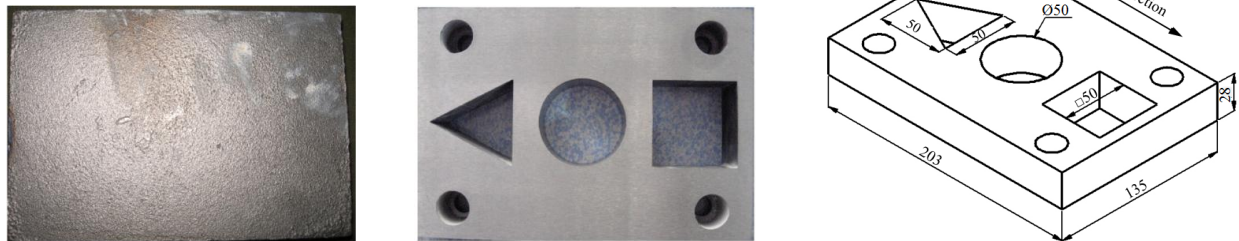


Fig. 2 The cast sample, machined surface, dimensions of the specimen used in the experiment (dimensions in mm)

In order to determine which wheel and grinding parameters influence the shape error in circle geometry, a number of experiments were conducted. To understand the characteristic of the shape error in circle geometry, wheel speed, coolant flow rate, spark out, workpiece, geometry and dimensions are constant. Although many factors affect the grinding process, some of the independent parameters such as wheel grain size ( $M$ ), grinding depth ( $D$ ), table speed ( $V$ ) and cross feed ( $W$ ) were taken into account. Therefore, the  $L_{16}(4^4)$  orthogonal array was selected for this study. The selected process parameters and their levels have been shown in Table 2.

An experimental design, measured shape error in circle geometry ( $CE$ ) and the calculated  $S/N$  ratios are shown in Table 3.

#### 4. Measurement of shape error

In order to determine the shape errors of the workpieces, the Opto-TOP HE 3D white light scanning system was used. The measuring principle is characterized by determining the order and phase of the fringe pattern projected onto the object surface and imaged by the camera. The light and dark fringes on the surface of the body are deformed depending on the surface shape. The coded lights are directed towards the surface of the workpiece to have a special angle. This angle is called as triangulation. A special algorithm then performs a triangulation calculation to measure the exact position of each point within the fringe pattern, covering up to a million points for each scan. A wire frame model was generated and, finally, texture mapping was done by means of the digital images and the RapidForm software. The CAD data set generated on the basis of the scan data can be directly compared with the

Table 2

Process parameters and their levels

Process parameters	Levels			
	1	2	3	4
(M) Wheel grain size, mesh	36	46	60	80
(D) Grinding depth, $\mu\text{m}$	10	25	40	55
(V) Table speed, m/min	18	22	26	30
(W) Cross feed, mm	1	2	3	4

Standard  $L_{16}$  orthogonal array, measured shape error values and calculated signal to noise ratios ( $S/N$ )

Trial number	Factors					
	Wheel grain size, mesh	Grinding depth, $\mu\text{m}$	Table speed, m/min	Cross feed, mm	Shape error, $\mu\text{m}$	Signal to noise ratios, dB
1	36	10	18	1	33.23	-30.431
2	36	25	22	2	38.64	-31.741
3	36	40	26	3	52.62	-34.423
4	36	55	30	4	55.80	-34.933
5	46	10	22	3	34.62	-30.787
6	46	25	18	4	46.23	-33.298
7	46	40	30	1	40.85	-32.224
8	46	55	26	2	47.77	-33.583
9	60	10	26	4	41.58	-32.378
10	60	25	30	3	46.10	-33.274
11	60	40	18	2	39.61	-31.956
12	60	55	22	1	36.63	-31.277
13	80	10	30	2	33.06	-30.386
14	80	25	26	1	35.09	-30.904
15	80	40	22	4	34.92	-30.861
16	80	55	18	3	39.08	-31.839

scan data of the original. Also, digitization systems are used during the process of resolving as technological convenience. As a result of optical scanning, point cloud and polygon mesh data were obtained. Finally, the scanned data were registered into the CAD data to calculate and display the deviations of the two data sets by using the software [13, 14]. Fig. 3 shows a typical example of the surface obtained by optical scanning. The values of shape error of each workpiece are measured from the workpiece surface within a total length of a measured workpiece. The measurement of 30 points was taken from the scanned geometry. Here, the height difference between a maximum point and a minimum point of the ground surface was chosen as the values of shape error.

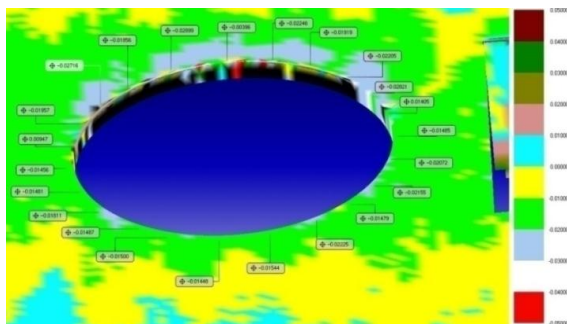


Fig. 3 A typical example of surface obtained by optical scanning

## 5. Experimental results and discussion

### 5.1. Analysis of the $S/N$ ratios

In the Taguchi method, the term “signal” ( $S$ ) represents the desirable value (mean) for the output characteristic and the term “noise” ( $N$ ) represents the undesirable value for the output characteristic. Taguchi uses the  $S/N$  ratio to measure the quality characteristic deviating from the desired value. Process parameter settings with the highest  $S/N$  ratio always yield the optimum quality with minimum variance [15, 16]. The results of square and triangular geometry are not included in this study, another study presented. The standard commercial statistical soft-

ware package Minitab 15.0 was used in the analysis of results. Fig. 4 shows plots of the  $S/N$  response graphs for the four factors studied at four levels for the shape error in circle geometry. On the other hand smaller-the-better quality characteristic for shape error should be taken for obtaining optimal grinding performance.

As can be seen Fig. 4, the preference value for the wheel grain size of wheel is 80 mesh is better than 36, 46 and 60 mesh. This is because wheel grain size of 80 mesh has relatively fine grits than the other wheel grain size (36, 46 and 60 mesh). A decrease in the particle size of abrasive grain increases the grain size of wheel, which can cause better surface finish. This improvement in surface quality with the fine grits was due to reduction in maximum chip thickness at lower grit size. As regards the grinding depth, 10  $\mu\text{m}$  less shape error than 25, 40 and 55  $\mu\text{m}$ . Fig. 4 shows that shape error increases as grinding depth increases. This increase in shape error is expected because of increased chip thickness at higher grinding depth. As to the table speed, among the four values investigated, 22 m/min is the best selection, followed by 18, 26 and 30 m/min. In other words, it was observed that up to a level 2 value of table speed, the shape error decreases but from that level on, it increases. It is known that surface quality decreases with increased table speed. Based on the analysis of  $S/N$  ratio, the minimum shape error was obtained at 22 m/min table speed. This result seems to conflict with the general rules. However, there are similar fluctuations in the literature [9, 10]. Eventually, this fluctuation was due to the compositions of the stiffness of the machine system and wheel/workpiece contact pressure. Finally, the preference values for cross feed 1 mm are better than 2, 3, and 4 mm. It is evident that the shape error increases with increasing grinding depth and cross feed, but it decreases with increasing grain size of wheel. And also maximum  $S/N$  response value at each level has given the minimum shape error.

Optimum level is the selection of appropriate values in the wheel and grinding parameters in order to minimize the shape error in geometry of circles. Based on  $S/N$  ratio value, the optimal grinding performance for the shape error was obtained at wheel grain size of 80 mesh (level 4),

10 μm grinding depth (level 1), 22 m/min table speed (level 2) and 1 mm cross feed (level 1). Experimental results concluded that the shape error does not completely disappear, but can be estimated and controlled by grinding parameters.

The ANOVA can be used to test the adequacy of the developed models at 95% confidence level. Table 4 presents the results of ANOVA for shape error in inter-

rupted grinding. From Table 4, it is apparent that the  $F$  values of parameters wheel grain size, grinding depth, table speed and cross feed were all greater than  $F_{0.05,3,3} = 9.28$ . Hence, this indicates that the all the factors (wheel grain size, grinding depth, table speed and cross feed) are significant in affecting the shape error in circle geometry. Wheel grain size was found to be the major factor affecting the shape error in all control parameters.

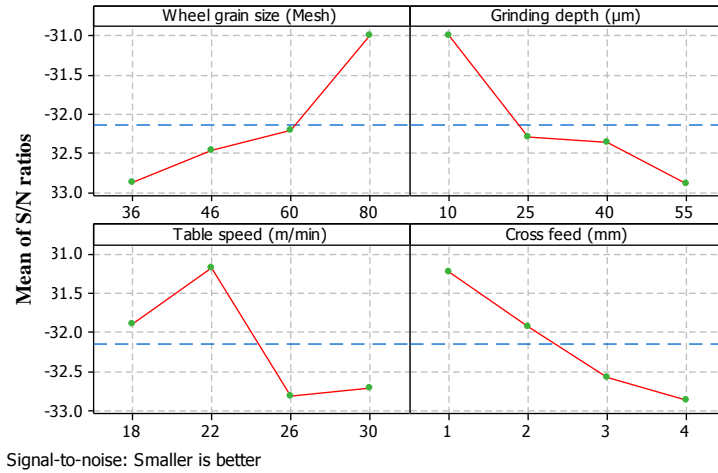


Fig. 4 Effect of wheel and grinding parameters on shape error

ANOVA results show the significance of factors on the shape errors

Table 4

Source of variation	Degree of freedom	Sum of squares	Variance	$F$ - ratio	$F$ - tab	Percent %
$M$	3	193.177	64.392	19.03	9.28	26.83
$D$	3	179.099	59.700	17.64	9.28	24.88
$V$	3	178.128	59.376	17.55	9.28	24.74
$W$	3	159.364	53.121	15.70	9.28	22.14
Error	3	10.150	3.383	-	-	1.41
Total	15	719.918	-	-	-	100

Percent (%) is described as the significance rate of the process parameters on the shape error. The order of significance of these parameters is wheel grain size (26.83%), grinding depth (24.88%), table speed (24.74%) and cross feed (22.14%) respectively in the grinding of GS-C25 cast steel (Fig. 5).

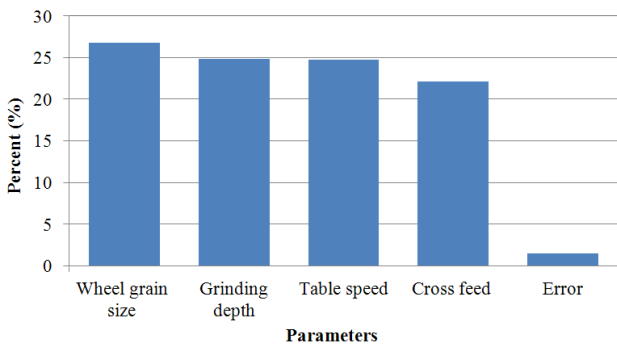


Fig. 5 Percentage contribution of parameters on shape error

5.2. Determination of optimum processing conditions

Verification experiment was carried out by utilizing the experimental condition of the four factors as: wheel grain size of 80 mesh, 10 μm grinding depth, 22 m/min

table speed and 1 mm cross feed ( $M_4D_1V_2W_1$ ) for the minimum shape error in circle geometry obtained through optimization process. To maintain the same experimental conditions, the dimension and shape for confirmation experiment was kept constant during the interrupted grinding. Table 5 shows the results of the experimental confirmation using their optimal grinding parameters. As it is shown in Table 5, the shape error is decreased from 39.61 μm to 21.01 μm. This means that the value of the shape error is decreased about 1.88 times. It obviously demonstrates that the shape error is greatly improved through this approach. In the comparison of the predicted shape error with actual shape error using the optimal grinding parameters, appropriateness is observed between the estimated and verified shape error.

Table 5

Results of the verified experiment for shape error

	Initial grinding parameters	Optimal grinding parameters	
		Prediction	Experimental
Setting level	$M_3D_3V_1W_2$	$M_4D_1V_2W_1$	
Shape error, μm	39.61	20.844	21.01

Improvement for shape error = 18.6 μm.

### 5.3. Development of linear shape error mathematical model

In the present study, multiple regression analysis is performed to find out the relationship between grinding independent variables and shape error. Grain size of the wheel, grinding depth, table speed and cross feed were considered as variables in the development of mathematical models for shape error. Shape error can be expressed as follows:

$$CE = f(M, D, V, W) \quad (1)$$

where  $CE$  is the desired response and  $f$  is the response function. The linear model of shape error can be written as follows

$$CE = b_0 + b_1A + b_2B + b_3C + b_4D + \varepsilon \quad (2)$$

where  $b_0$  is constant,  $b_1$ ,  $b_2$ ,  $b_3$  and  $b_4$  represent the coefficients and  $\varepsilon$  is the error. Eq. (2) can be rewritten according to the four variables ( $M$  - grain size of wheel,  $D$  - grinding depth,  $V$  - table speed and  $W$  - cross feed) in the coded form

$$CE = b_0 + b_1M + b_2D + b_3V + b_4W + \varepsilon \quad (3)$$

The developed mathematical model for the estimation of the shape error in surface grinding is expressed in coded units as follows

$$CE = 26.7 - 0.207M + 0.187D + 0.533V + 2.79W + \varepsilon \quad (4)$$

In multiple linear regression analysis,  $R^2$  is the correlation coefficient ( $R^2 > 0.80$ ) for the models, which indicate that there is a good agreement between the experimental data and created model. In this study,  $R^2$  is found as 0.822 of the value which is larger than (0.8). As it is seen from this, the regression model for shape error matches fairly good the experimental data. In other words, the  $R^2$  values indicate that the predictors explain 82.2% of the variance in shape error. It could be seen from the developed model that geometric error decreases with the increase in wheel grain size, but increase with the increase the grinding depth, table speed and cross feed. Using the above model, the shape error according to various grinding conditions could be predicted and minimized easily. For each experiment parameters, the developed model has been used to predict the shape error for the each experiment.

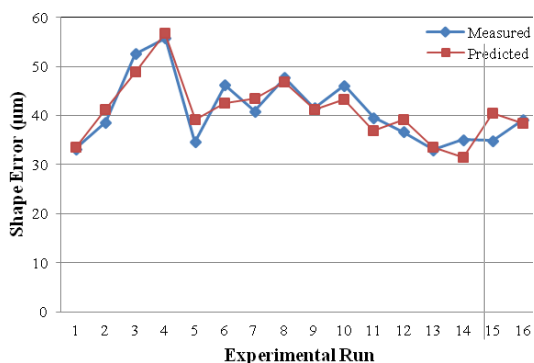


Fig. 6 Comparison of measurement and predicted results

The obtained results and comparison with

experimentally measured results has been shown in Fig. 6. Comparing the shape error obtained from modeled and experimental values little variation was observed.

## 6. Conclusions

The influence of wheel and cutting parameters, such as grain size of the wheel, grinding depth, table speed and cross feed on shape error of cast steel were investigated experimentally and statistically. Taguchi method was employed in the optimization of the process parameters. The following conclusions may be drawn from present study:

1. The shape error can be decreased by increasing grain size of the wheel, and decreasing the grinding depth and cross feed.
2. The best parametric combination of the four control factors for minimizing the shape error is  $M_4D_1V_2W_1$ , which means that grain size of wheel is 80 mesh, grinding depth is 10  $\mu\text{m}$ , table speed is 22 m/min and cross feed is 1 mm.
3. The results of statistics for the grinding indicated that the wheel grain size, grinding depth, table speed and cross feed have the influence on shape error by 26.83%, 24.88%, 24.74% and 22.14% respectively.
4. Optimized cutting conditions substantially reduce shape error from 39.61 to 21.01  $\mu\text{m}$ .
5. There is a good agreement between the experimental data and developed model. Because of these a multiple regression model can be used to predict shape error in grinding.

## Acknowledgements

The authors are very grateful to Defne Engineering for optical measurements.

## References

1. Ostaševičius, V.; Ubartas, M.; Gaidys, R.; Jūrėnas, V.; Samper, S.; Daukševičius, R. 2012. Numerical-experimental identification of the most effective dynamic operation mode of a vibration drilling tool for improved cutting performance, *Journal of Sound and Vibration* 331(24): 5175-5190. <http://dx.doi.org/10.1016/j.jsv.2012.07.007>.
2. Gavas, M.; Karacan, İ.; Kaya, E. 2011. A novel method to improve surface quality in cylindrical grinding, *Exp. Techn.* 35(1): 26-32. <http://dx.doi.org/10.1111/j.1747-1567.2009.00575.x>.
3. Tsai, H.H.; Hocheng, H. 1998. Analysis of transient thermal bending moments and stresses of the workpiece during surface grinding, *J. Thermal Stress* 21(6): 691-711. <http://dx.doi.org/10.1080/01495739808956169>.
4. Tsai, H.H.; Hocheng, H. 1998. Investigation of the transient thermal deflection and stresses of the workpiece in surface grinding with the application of a cryogenic magnetic chuck, *J. Mater. Process. Technol.* 79(1-3): 177-184. [http://dx.doi.org/10.1016/S0924-0136\(98\)00008-9](http://dx.doi.org/10.1016/S0924-0136(98)00008-9).
5. Tsai, H.H.; Hocheng, H. 2001. Monitoring strategy of thermal-induced convex deformation of workpiece in

- surface grinding, *Int. J. Adv. Manuf. Technol.* 17(10): 710-714.  
<http://dx.doi.org/10.1007/s001700170115>.
6. **Tsai, H.H.; Hocheng, H.** 2002. Prediction of a thermally induced concave ground surface of the workpiece in surface grinding, *J. Mater. Process. Technol.* 122(2-3): 148-159.  
[http://dx.doi.org/10.1016/S0924-0136\(01\)01059-7](http://dx.doi.org/10.1016/S0924-0136(01)01059-7).
  7. **Tsai, H.H.; Hocheng, H.** 2002. On-line identification of thermally-induced convex deformation of the workpiece in surface grinding, *J. Mater. Process. Technol.* 121(2-3): 189-201.  
[http://dx.doi.org/10.1016/S0924-0136\(01\)01058-5](http://dx.doi.org/10.1016/S0924-0136(01)01058-5).
  8. **Kagiyada, T.; Kanauchi, T.** 1985. Three-dimensional thermal deformation and thermal stress in workpieces under surface grinding, *J. Thermal Stress.* 8(3): 305-318.
  9. **Kwak, J.S.** 2005. Application of Taguchi and response surface methodologies for geometric error in surface grinding process, *Int. J. Mach. Tools. Manuf.* 45(3): 327-334.  
<http://dx.doi.org/10.1016/j.ijmachtools.2004.08.007>
  10. **Kwak, J.S.; Kim, I.K.** 2006. Parameter optimization of surface grinding process based on Taguchi and response surface methods, *Key Eng. Mater.* 306-308: 709-714.  
<http://dx.doi.org/10.4028/www.scientific.net/KEM.306-308.709>.
  11. **Ohmori, H.; Dai, Y.; Lin, W.; Suzuki, T.; Katahira, K.; Itoh, N.; Makinouchi, A.; Tashiro, H.** 2003. Force characteristics and deformation behaviors of sintered SiC during an ELID grinding process, *Key Eng. Mater.* 238-239: 65-70.  
<http://dx.doi.org/10.4028/www.scientific.net/KEM.238-239.65>.
  12. **Sosa, A.D.; Echeverria, M.D.; Moncada, O.J.; Sikora, J.A.** 2007. Residual stresses, distortion and surface roughness produced by grinding thin wall ductile iron plates, *Int. J. Mach. Tools. Manuf.* 47(2): 229-235.  
<http://dx.doi.org/10.1016/j.ijmachtools.2006.04.004>.
  13. <http://www.defnemuhendislik.com/en.html>. 2010.
  14. **Peipe, J.; Przybilla, H.J.** 2005. Modeling the Golden Madonna. CIPA 2005 XX International Symposium, Torino, Italy. 934-936.
  15. **Palanikumar, K.** 2008. Application of Taguchi and response surface methodologies for surface roughness in machining glass fiber reinforced plastics by PCD tooling, *Int. J. Adv. Manuf. Technol.* 36(1-2): 19-27.  
<http://dx.doi.org/10.1007/s00170-006-0811-0>.
  16. **Kurt, M.; Bagci, E.; Kaynak, Y.** 2009. Application of Taguchi methods in the optimization of cutting parameters for surface finish and hole diameter accuracy in dry drilling processes, *Int. J. Adv. Manuf. Technol.* 40(5-6): 458-469.  
<http://dx.doi.org/10.1007/s00170-007-1368-2>.

M. Kurt, U. Köklü

## FORMOS PAKLAIDŲ MAŽINIMAS TRŪKIAME ŠLIFAVIMO PROCESE TAIKANT TAGUŠI METODĄ

### R e z i u m e

Formos paklaidų atsiranda trūkiame paviršiuje šlifavimo proceso metu. Šiame darbe yra ištirta šlifavimo disko grūdelių dydžio, šlifavimo gylis, stalo greičio ir skersinės pastūmos įtaka formos tikslumui trūkiaus šlifavimo atveju. Eksperimentiniams tyrimams pasirinktas liejamasis plienas GS-C25. Variantų analizės metodu atliktas disko ir pjovimo parametrų įtakos formos paklaidų rinkinio bei signalo ir triukšmo santykio įvertinimas. Variantų analizės rezultatai parodė, kad procesui daugiausia įtakos turi disko grūdelių dydis, šlifavimo gylis, stalo greitis ir skersinė pastūma. Įvertintos ir išmatuotos reikšmės yra gana artimos viena kitai, kas rodo, kad taikant regresinę analizę sukurtas modelis gali būti efektyviai panaudotas formos paklaidoms šlifuojant nuspėti.

M. Kurt, U. Köklü

## MINIMIZATION OF THE SHAPE ERROR IN THE INTERRUPTED GRINDING PROCESS BY USING TAGUCHI METHOD

### S u m m a r y

Shape errors appear around the interrupted surface in the grinding process. In this paper, the effect of wheel grain size, grinding depth, table speed and cross feed on shape error in interrupted grinding were investigated. GS-C25 cast steel material was selected as the workpieces materials to conduct experiments. In order to evaluate the wheel and cutting parameters on the shape error an orthogonal array, the signal-to-noise ratio, the analysis of variance and multiple regression analyses were applied. The analysis of variance results indicated that the most significant process parameters are wheel grain size followed by grinding depth, table speed and cross feed. As a result, the predicted and measured values were fairly close each other, which indicate that the developed model using the regression analysis can be effectively used to predict the shape error in grinding.

**Keywords:** Interrupted grinding, Shape error, Taguchi method.

Received September 26, 2011

Accepted November 15, 2012